The International Journal of Advanced Manufacturing Technology (2018) 97:2489–2499
https://doi.org/10.1007/s00170-018-2102-y

ORIGINAL ARTICLE

Mechanical and thermal properties of friction-stir welded joints of high density polyethylene using a non-rotational shoulder tool

Mirley Moreno-Moreno[1] · Yorledis Macea Romero[1] · Habib Rodríguez Zambrano[2] · Nora Catalina Restrepo-Zapata[3] · Conrado Ramos Moreira Afonso[4] · Jimy Unfried-Silgado[5]

Received: 27 October 2017 / Accepted: 2 May 2018 / Published online: 15 May 2018

Abstract
The effects of rotational and welding speed on the mechanical properties and thermal behavior in friction stir welded joints of high-density polyethylene using a non-rotational shoulder have been investigated experimentally. Tensile properties and hardness were measured to determine the mechanical properties, and the effect of the welding parameters. Heating and cooling cycles of differential scanning calorimetry were used to establish thermal properties. Microstructure observations complemented experimental observations. Results showed that tensile strength, hardness, and crystallinity decreased when rotational speed was increased, while the welding speed effect was weak. Deleterious phenomena on molecular structure of the stir region were explained by means combination of selected welding parameters and the material flow during the process.

Keywords Polyethylene · Molecular structure · DSC · Tensile strength test · Friction-stir welding

1 Introduction

Friction stir-welding (FSW) is performed using a non-consumable rotating tool, which has two key parts: shoulder and pin, as shown in Fig. 1. As pointed out by Nandan et al. [1], and Mishra et al. [2], these two parts (which are in contact with the material that is being welded) are responsible for generating heat, extruding, and forging the material until its confinement. Welded joint consolidation is possible through frictional heat, plasticizer heat, and material flow. Rajamanickam et al. [3], and Thomas et al. [4], established that the most relevant process parameters in FSW are rotational speed (ω), welding speed (v_s), downward force (F_Z), and applied torque (τ).

As discussed by Threadgill et al. [5], because FSW is a solid-state process, by using this technique, it is possible to avoid problems related to state changes such as solidification, porosity, liquation, and hot cracking in metals. According to Throughton [6], this advantage (a solid-state process) is a significant characteristic that is highly desirable, especially for welding polymers. However, polymers have substantial differences in physical and mechanical properties in comparison to metals; for example, caused by the weak bond between large molecular chains, polymers have lower melting temperature.

Polyethylene (PE) is the most used polyolefin thermoplastics due to its durability, flexibility, and toughness. Peacock [7] reported that PE has excellent properties such as high environmental stress crack resistance, high stiffness, high chemical and corrosion resistance, light weight, and low fabrication and maintenance costs. Vijayan et al. [8] determined that thermoplastics (including PE) usually are welded using processes that involve some of the following condition: heat conduction (heated wedge, socket, and hot gas welding), heat radiation (which uses electromagnetic radiations, such as laser welding), and mechanical friction (ultrasonic, vibration, and rotation welding). FSW belongs to the last group (mechanical friction). On one hand, Lai et al. [9], who investigated on the

✉ Jimy Unfried-Silgado
jimyunfried@correo.unicordoba.edu.co

[1] Facultad de ingeniería, Programa de ingeniería mecánica, Grupo IMTEF, Universidad Autónoma del Caribe, Barranquilla, Colombia

[2] División de Ingeniería, Grupo GIMYP, Universidad del Norte, Barranquilla, Colombia

[3] Núcleo de Matemáticas, Física y Estadística, Facultad de Ciencias, Universidad Mayor, Santiago, Chile

[4] Departamento de Engenharia de Materiais – DEMA, Universidade Federal de São Carlos, São Carlos, SP, Brazil

[5] Departamento de Ingeniería mecánica, Grupo ICT, Universidad de Córdoba, Cr 6 No. 76-103, Montería, Colombia

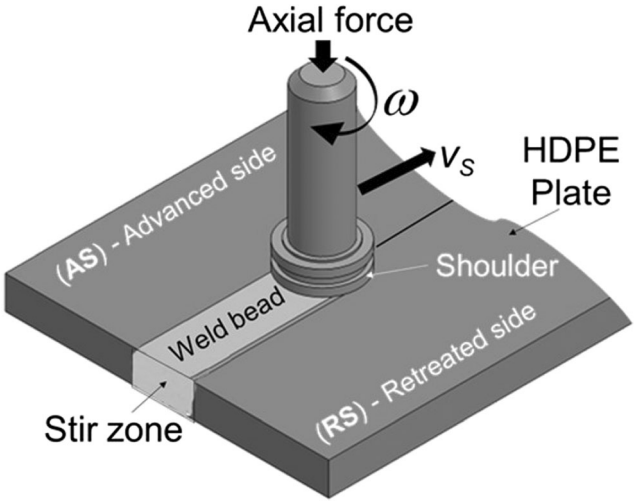

Fig. 1 Sketch of friction stir-welding showing parameters and parts

weldability of PE using electron beam irradiation and butt fusion welding, showed that even under suitable conditions, imperfections (such as voids and crystal orientation changes) are present in the welded joints. Besides, Leskovics et al. [10] have reported loss of ductility in FSW joints, which indicates that the presence of imperfections in combination with a reduction of ductility leads to significant detriment in mechanical properties. Considerable modifications in crystal orientation and crystallinity percent are also expected, as it has been reported by Li et al. [11], as well as a reduction in lifetime expectation, as it was observed by Grewell et al. [12]. Therefore, substantial efforts have been recently made to understand the effects of the most relevant parameters (ω, v_s, F_Z, τ, and tool design) on mechanical properties of FSW joints. Kiss and Czigany [13] investigated the effect of rotational and welding speed on FSW joints of PE. In their work, the authors evaluated the applicability of FSW in polymers utilizing tensile tests and differential scanning calorimetry (DSC). They found that welded joints suffer embrittlement due to non-homogenization, and it is related to a reduction in crystallinity within the welded regions. Hoseinlaghab et al. [14] studied the effects of rotational and welding speed, tool geometry, and tilt angle on creep properties of FSW joints in PE. They observed a relative independence between process parameters and pin geometry, obtaining best weld quality and creep properties using a pin with cylindrical geometry. Bozkurt [15] investigated by means of Taguchi's optimization model the influence of process parameters on the tensile properties of FSW joints in PE. He concluded that the rotation speed is the most important process parameter that affects mechanical properties of FSW joints in PE. Nateghi and Hosseinzadeh [16] studied the effect of assisted cooling nugget during FSW of PE. The results showed that angular distortion, residual stress, and tensile strength of FSW joints are improved using assisted cooling. Azarsa and Mostafapour [17] studied flexural strength in FSW of high-density polyethylene (HDPE) sheets under the influence of the process parameters (rotational and welding speed) and tool temperature. These authors used a non-rotational (stationary) shoulder tool with heating control. Flexural strength in HDPE welded joints displayed best results with a higher rotational speed, lower welding speed, and shoulder temperature at 100 °C.

Banjare et al. [18] used a new non-rotational shoulder tool with heating assistance to enhance surface finish and to reduce material loss and chip formation during FSW for several thermoplastics, including PE. Results showed that ductility and tensile strength of welded joints were improved, compared to conventional tools for FSW joints. Vijendra and Sharma [19] investigated FSW in PE using a new tool design with a pin heated by induction. At 45 °C (tool-pin temperature), a tensile strength similar to the base material was obtained, but its hardness decreased. Also, by means of DSC, a high level of crystallization in the stir zone was observed. Simões and Rodrigues [20] investigated material flow and thermomechanical conditions during FSW of polymers. These authors found that the differences between pin and shoulder driven flow could explain the formation of important discontinuities and weldability problems in polymer welding. Non-rotational shoulder tools have the advantages of reducing thermal transfer to welded joint, obtaining higher tensile strength, and minimizing a serious problem named "root defect" in FSW of thermoplastics [21]. Due to excessive heating and the application of uncontrolled parameters during thermoplastics of FSW, the current work aims to study the influence and inter-relationships of process parameters on mechanical and thermal properties in friction stir welding of HDPE using a non-rotational (stationary) shoulder tool without heating assistance.

2 Experimental procedure

2.1 Materials

HDPE plates of 246 mm × 60 mm × 8.5 mm were used as base material. The plates were acquired commercially and were fabricated by extrusion from recycled material. The extrusion

Table 1 Physical properties of HDPE determined experimentally

Physical Properties	T_g (°C)	T_m (°C)	ΔH_f (J g^{-1})	χ_c (%)
Experimental	− 127.6	131.3	194.8	67.2

Table 2 Chemical composition of AISI H-13 steel

Element	Fe	C	Cr	Mn	Si	V	Mo
wt%	Bal.	0.34	5.2	0.4	1.1	0.95	1.4

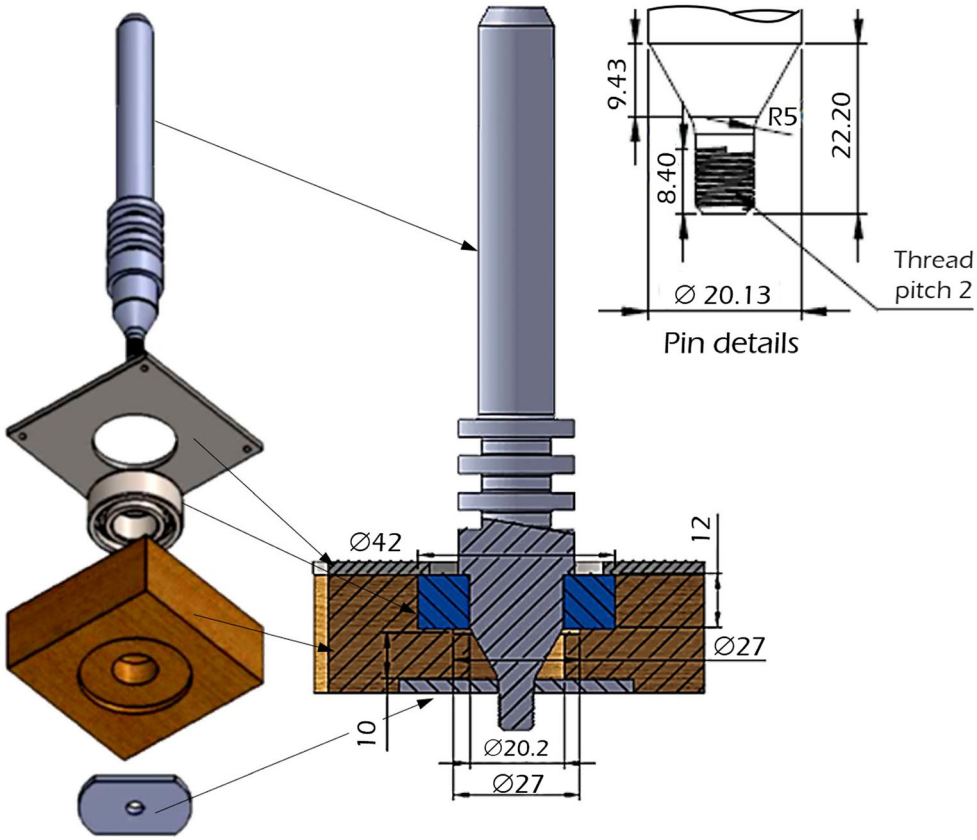

Fig. 2 Tool dimensions and geometry

orientation was traced to carry out the welding process perpendicularly to this direction. Table 1 summarizes the most important properties of the HDPE used in the study.

2.2 Tool design

A non-rotational shoulder tool was used to perform the welds [21]. This kind of tool was selected to reduce heat transfer between tool surface and the stirred zone of the welded joint [22]. The tailored FSW tool consisted of a steel monolithic body with a cylindrical threaded pin (as shown in Fig. 2), a ball bearing, a wood scraper, and a support ring-wing made of bronze. Tool dimensions and geometry are shown also in Fig. 2. The tool body was fabricated of AISI H13 steel (see Table 2), which was heat-treated until to reach 58 Rockwell hardness C; meanwhile, the scraper was made of pinewood. The ring-wing was designed without a heating assisted device.

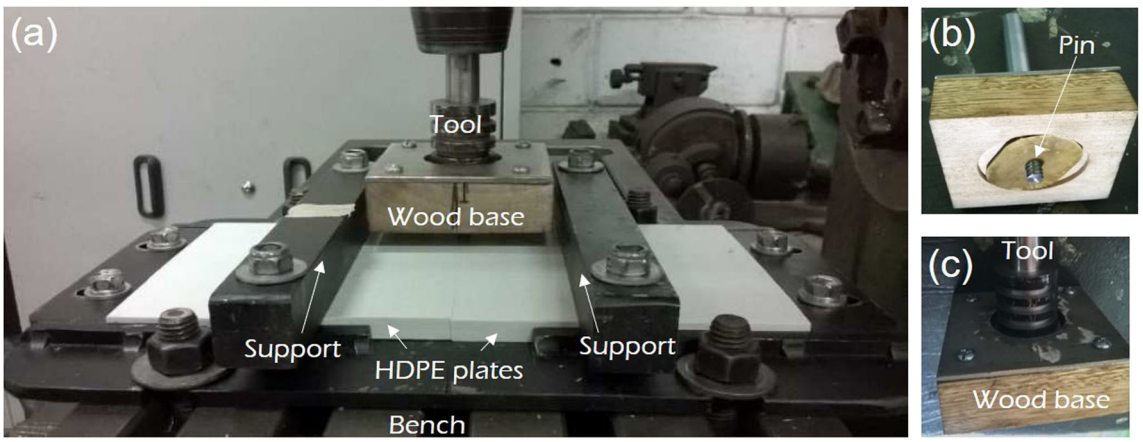

Fig. 3 HDPE plates clamped on the bench of the milling machine using a specially designed support. **a** General view of support. **b** Ring-wing. **c** Wood scraper

Table 3 Process parameters range selected to evaluate FSW in HDPE

Rotational speed ω (rpm)	1036	846
Traverse speed v_s (mm min^{-1})	14	25

2.3 Experiment setup

A conventional milling machine (Imomill®) of 3.2 HP was used to weld the joints. The tailored tool was properly engaged into the tool-holder of the machine. HDPE plates were clamped on the bench of the milling machine using a specially designed support, which is shown in Fig. 3. The plates were attached to the support by means of two bolted beams of AISI/SAE 1045 steel, restricting movement in all directions without deforming or bending the plates. Rotational speed was adjusted taking into consideration the available gearbox combinations of the milling machine, and it was measured using a tachometer. The bench's displacement and a calibrated chronometer were used to measure welding speed during welding.

2.4 Process parameter selection and performance

In this work, the process window has been limited up to 1200 rpm for rotational speed, and up to 45 mm min^{-1} for welding speed in accordance to a previous work [23]. Based on the prior information, selected process parameters were limited to values allowed by the milling machine, viz., $800 < \omega < 1100$ rpm, and $14 < v_s < 25$. The selected velocities also fulfilled with the values recommended in [14, 16], i.e., $\omega < 910$ rpm and $v_s < 44$ mm min^{-1} to avoid extensive local fusion of material and discontinuities during FSW of HDPE. Tool tilt angle was 0° and the axial load was not recorded during test, maintaining constant these values during tests. A first approach to select the process parameters was developed using the rotational and welding speed ranges shown in Table 3. Two samples were obtained for each combination of parameters. Non-destructive and destructive tests were performed to evaluate the soundness of the welded joints. The criteria used for selection of optimal conditions of welding were (i) the presence of burrs with height > 2 mm, (ii) presence of discontinuities with length > 10 mm, (iii) presence of pin-hole defects, and (iv) presence of porosity or voids in the weld surface. Two levels of each parameter were selected to run a statistical experimental design. A 2^k factorial design was applied to evaluate the influence of process parameters on crystallinity and tensile strength [24]. The experiments were carried out, and the tests were replicated three times for reliability within 5%.

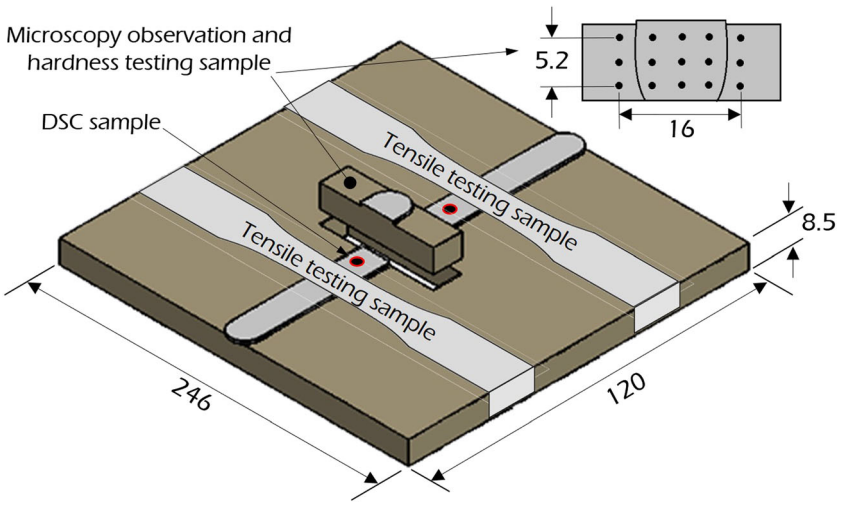

Fig. 4 Location of mechanical properties, microscopy observation and DSC testing samples

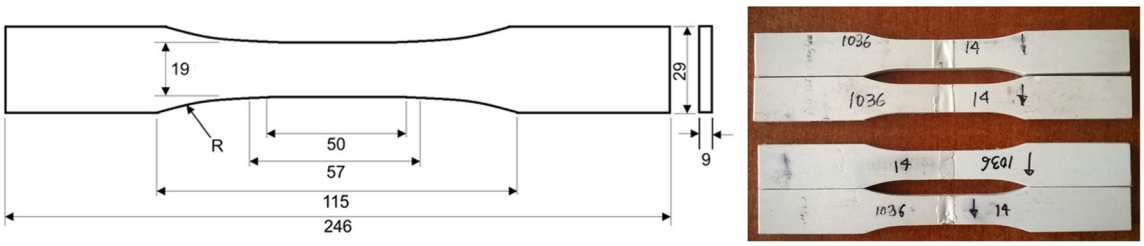

Fig. 5 Tensile testing sample

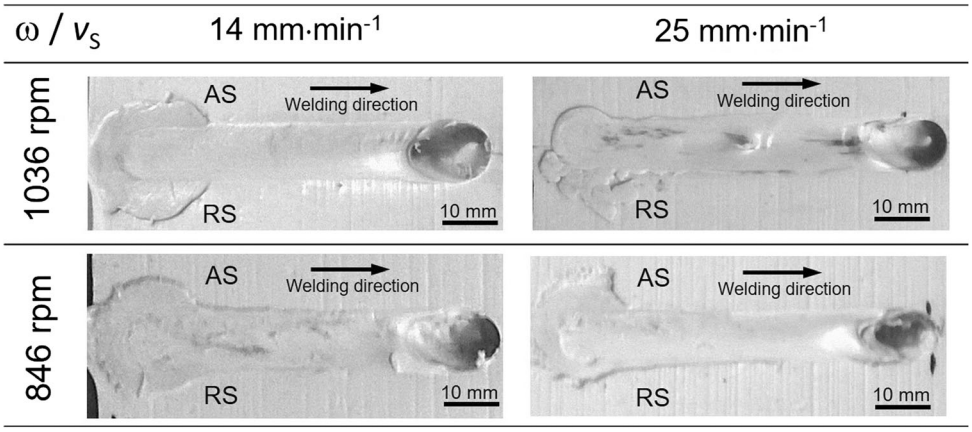

Fig. 6 Images show details of preliminary welded joints

2.5 Differential scanning calorimetry testing

Differential scanning calorimetry DSC analyses were carried out using a Netzsch® DSC 200 F3 calorimeter. Cold cut samples of 5 mg were extracted from the stirred region, as well as the base material of each welded joint used in the final experiments, as shown in Fig. 4. Samples were analyzed by means of DSC performing 2 cycles using a heating-cooling-heating rate of 10 K min^{-1} and a nitrogen N_2 flux of 50 ml min^{-1}. Welded region crystallinity χ was estimated for each DSC scan cycle using Eq. (1) as a function of melting enthalpy ΔH.

$$\chi = {}^{\Delta H_m}/_{\Delta} H_m^0 \quad (1)$$

where ΔH^0_m is a reference value corresponding to the fusion heat of 100% crystalline HDPE, and ΔH_m (J g^{-1}) is the melting enthalpy of the studied region of HDPE welded joint. The reference value of ΔH^0_m is 290 J g^{-1} for this work, which was taken from [25].

2.6 Tensile test

Cross section tensile samples were extracted from welded joints according to the ASTM D 638-10 standard [26]. Figure 5 shows sample geometry and dimensions, and its location within the welded samples. The tensile tests were carried out in a universal testing machine (Shimadzu AG-1) with load capacity of 100 kN. Base material tensile testing specimens were extracted lying parallel, perpendicular, and 45° to the extrusion direction of the plates. These samples were

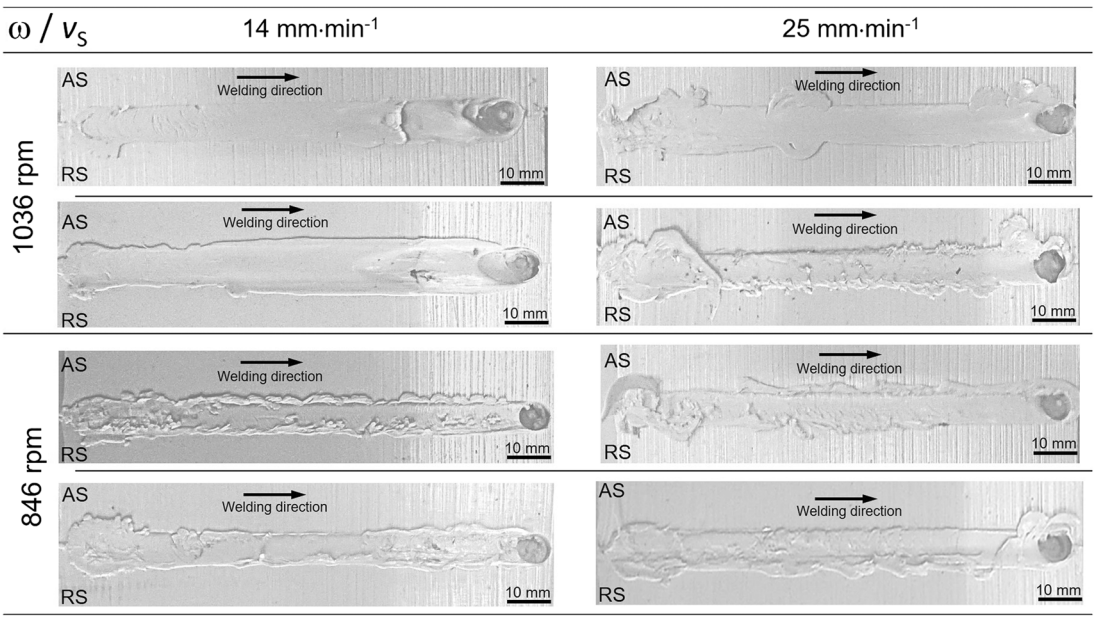

Fig. 7 Images show details of final welded joints

Table 4 Revolution pitch (R) for each combination of parameters

Rotational speed ω (rpm)	Traverse speed v_s (mm min^{-1})	Revolution pitch R (mm rev^{-1})
1036	14	0.0135
846	14	0.0165
1036	25	0.0241
846	25	0.0295

tested under the same conditions as the cross section tensile samples of the welds to compare results.

2.7 Welded joints characterization

Samples for microscopy observations were cut out from cross sections of welded joints, as shown in Fig. 4. Specimen preparation was done using sand papers with granulometry from 300 to 1500 per ASTM E2015-04. A confocal microscope Olympus® Lext 30 Measuring Laser Microscope OLS4100 and an optical stereoscope Leica® EZ4 HD were used for image analysis. Cross section hardness measurements of the welded joints were performed using a Shore-D durometer in accordance with ASTM D2240-05. Details on the location and distance between indentations are shown in Fig. 4.

3 Results and discussion

3.1 Process parameters selection and welded joints quality

Figure 6 shows details of the preliminary set of welded joints obtained using the selected process parameters. All samples displayed acceptable appearance, with smooth surfaces, free of internal discontinuities, and moderate burrs. A similar work has shown that selected process window and parameters used in this researcher provided temperatures in welded region between 130 and 180 °C [21]. These reached temperatures are near or higher than fusion temperature of PE; therefore, local fusion during welding process is susceptible to occur. The aforementioned agrees with appearance of softened surfaces of weld bead obtained in this work, concomitant result with use of static plain shoulder.

Details of the final welded samples are shown in Fig. 7. Compared to preliminary welded joints (see Fig. 6), final welded samples (Fig. 7) are longer. Therefore, thermal effects in final welded samples were more severe. Surface of weld bead was softer when higher rotational and lower welding speeds were used, which is coherent with higher heat input obtaining an apparently plain and homogeneity state of surface that included possible burrs. Nevertheless, welding speed variations did not have strong effect on the appearance of the welded joint surface. Welds obtained

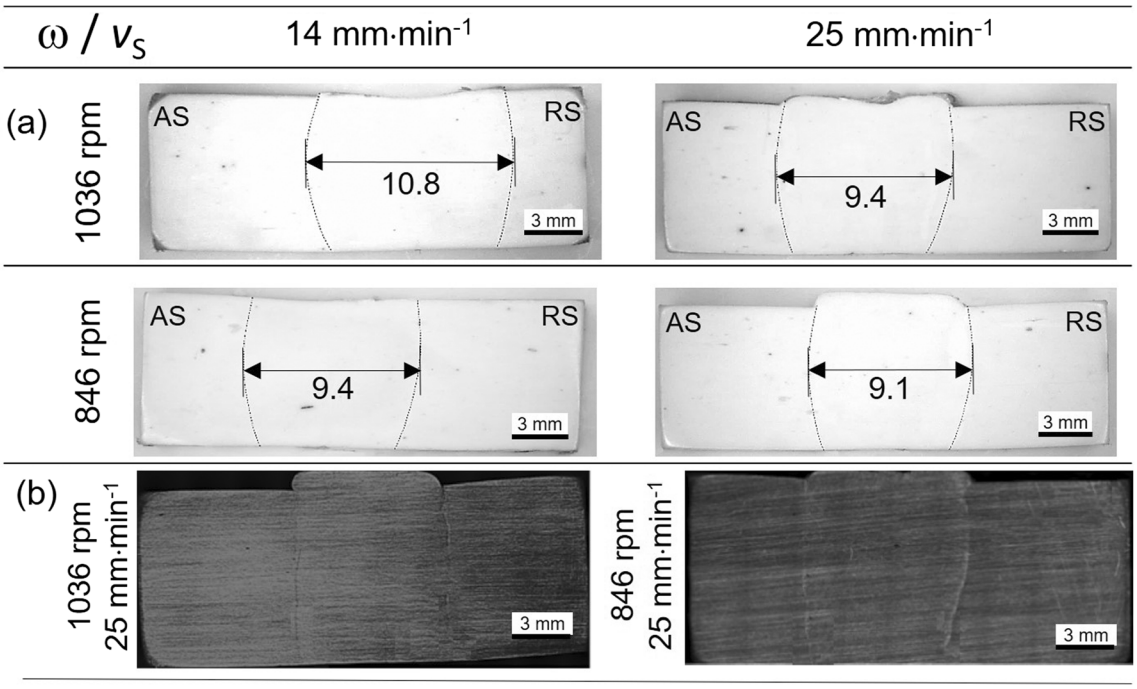

Fig. 8 Images showing cross sections of welded joints. **a** Optical microscopy. **b** Confocal microscopy

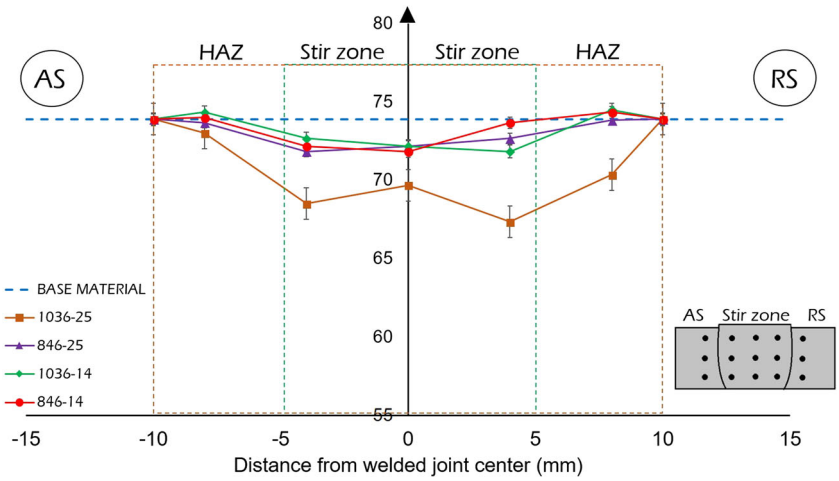

Fig. 9 Hardness testing results

using lower revolution pitch (R) showed the best appearance, as presented in Table 4.

Cross section macroscopic analysis evidenced that all welded joints were free of discontinuities, with moderate burr, and without appreciable reduction of the cross section area, as shown in Fig. 8a. Width of the welding joint was larger when rotational speed was increased, which is consistent with higher heat input, such as been discussed in other works [23]. Confocal microscopy analysis in Fig. 8b showed that welded joints had not voids and lack of fill along the joint. Absence of internal defects in welded joints leads to conclude that it is possible to expect low reduction of mechanical properties.

Table 5 Tensile properties of HDPE before welded

Properties	S_u (MPa)	S_p (MPa)	E (MPa)	ε (%)
Value	26.3	5.8	374.2	249.6

3.2 Hardness measurements

Shore-D hardness measurements of cross sections are shown in Fig. 9. Each curve corresponds to welds made with a different combination of process parameters, as indicated in Table 4. In general, hardness values were lower along whole of welding zones for all studied parameter combinations, as observed in other studies [19]. Aiming to distinguish each welding zone, in Fig. 9, has been established that the maximum stir zone width is 10 mm, which represents the average size of stir region observed in Fig. 8a. Thereby, the subjacent region outside of SZ and with lower hardness compared to the base material was defined as the heat-affected zone (HAZ). Microscopy observations were not clear to distinguish if the HAZ contents a region displaying simultaneously thermal effects and mechanical deformation, i.e., a true thermo-mechanically affected zone (TMAZ). However, later, it will be possible to associate the TMAZ existence with flow pattern of welding region.

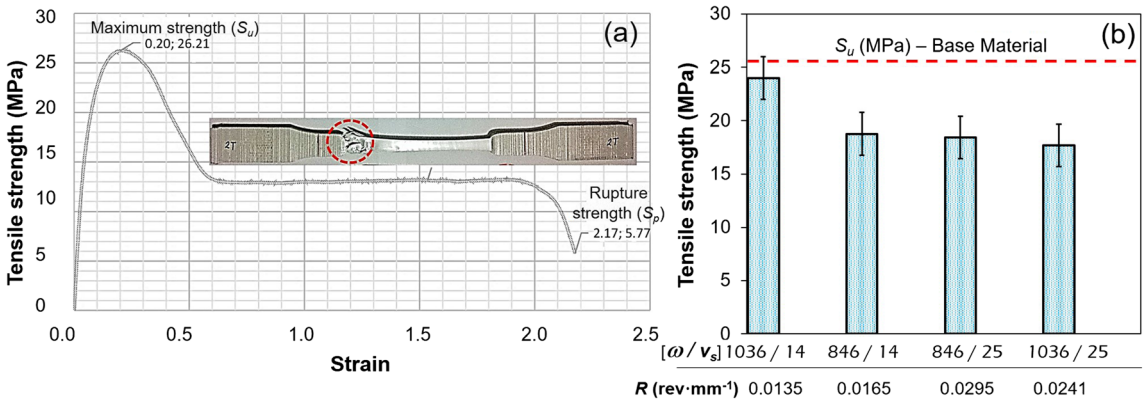

Fig. 10 Tensile strength results. **a** Strength vs. strain curve for the base material. **b** Effect of R (rev mm^{-1}) on the weld strength. ω in rpm and v_s in mm min^{-1}

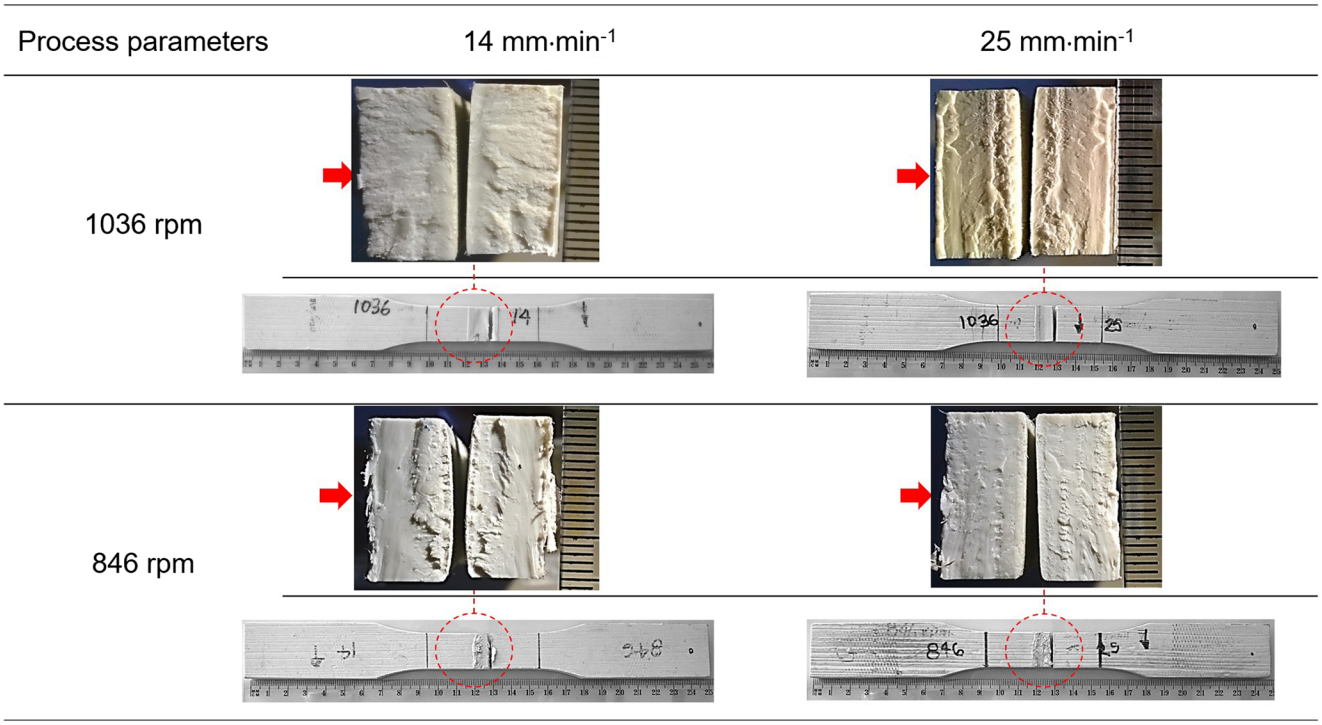

Fig. 11 Fracture surface appearance. Red arrows show retreating side of welded joints

It is expected to associate the hardness reduction in stir region with those process parameters that increase the heat input. The above is validated with the observation that the lowest hardness (~67 Shore-D) was obtained with the speed combination: 1036 rpm (rotational) and 25 mm min^{-1} (welding). A slight trend towards reduction of hardness was observed at the retreating side when rotational speed was increased. Hardness decreased around 10% within the stir zone, such as expected in FSW of HDPE using similar parameters and tool type [23].

Fluctuations of mechanical properties related to molecular structure changes are due to the differences in behavior of hardness in welded regions, given that the stir zone undergoes severe material flow because of stirring. Significant changes of direction, confinement, and cutting of molecular chains are usually expected. This leads to changes in molecular weight and appreciable reduction of ductility in the HDPE, as discussed in [23, 27]. The aforementioned fact was more marked at the retreating side of the welded joint. These changes on flow pattern direction in AS and RS side into SZ region could be associated to the presence of a TMAZ region in this kind of welded joints.

3.3 Tensile strength of welded joints and fracture behavior

Mean values of the tensile properties are summarized in Table 5. A typical stress vs. strain curve obtained in the tensile tests for the base material is presented in Fig. 10a. For the tensile tests of welded joints, the welds were oriented to be perpendicular to the extrusion direction, and the load was applied in the same extrusion direction. Figure 10b shows

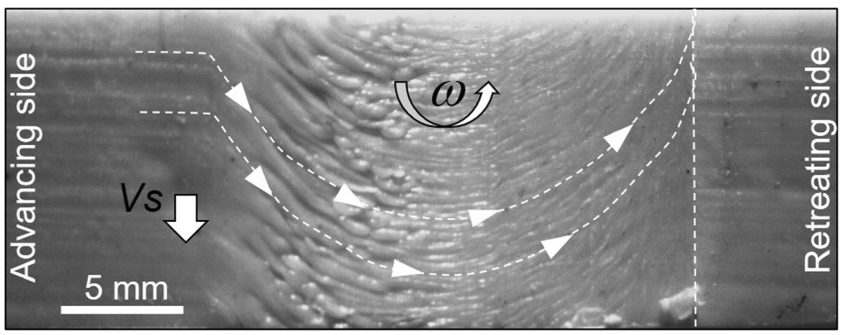

Fig. 12 Flow material behavior in welded samples

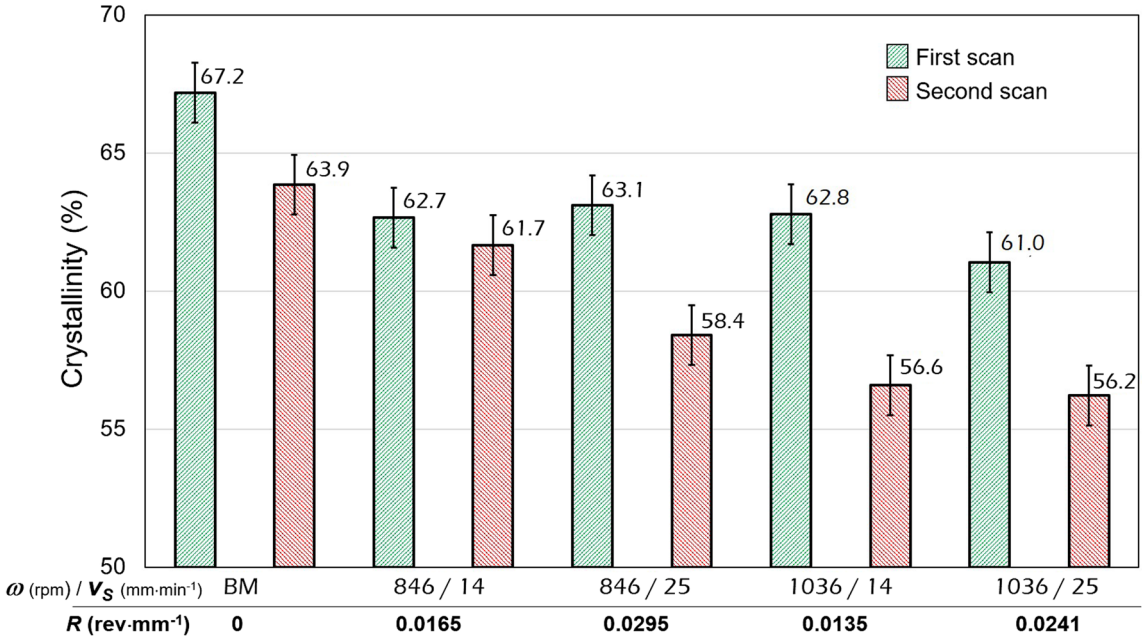

Fig. 13 DSC results show crystallinity in stir zone in function of welding parameters

mean values of the tensile results for the welded specimens. For the purpose of comparison with welded joint samples, only perpendicular tensile testing results of base material were used. While the base material samples displayed high plasticity in the tensile test, all welded samples displayed brittle fracture. The highest tensile strength (S_u) reached after fracture in the welded samples was lower than the one for the base material, as observed in [18, 28]. In general, S_u values are sensitive to revolution pitch (R) values so that S_u increases when R decreases, as it is shown in Fig. 10b, and discussed in other work [23]. Marginal plasticity was observed in the welded joints during tensile test exhibiting brittle fracture, no voids, and flat regions.

Fracture initiation was located at the retreating side in all samples, as observed in Fig. 11. A relationship between revolution pitch (R) and weld surface appearance was observed. When the R value decreases, the weld surface appears smoother and with fewer irregularities. This is consistent with hardness distribution in an inverse relationship, as observed in [23]. Lastly, it was observed that material flow affects the mechanical properties of welded samples. The fact that fractures initiated at the retreating side of all welded samples can be explained as consequence of thermal effects reducing material flow at this side is confirmed in [27]. These issues are related to the direction of the velocity vectors during the welding process, where an additive effect is expected at advancing side, as illustrated in Fig. 12. Consequently, a strong decrease in hardness was observed at the retreating side, more significant for high rotational speed.

The advancing side (AS) displays addition effects of welding and tangential velocity vectors that increase the amount of heat generated during the FSW process, while at the retreating side (RS), there is a subtraction effect. Therefore, the AS receives more heat than the RS, leading to lower cohesion in the RS, and molecular structure orientation is more affected [13], as shown in Fig. 12. Significantly greater changes in the flow pattern were observed on the RS compared to the AS.

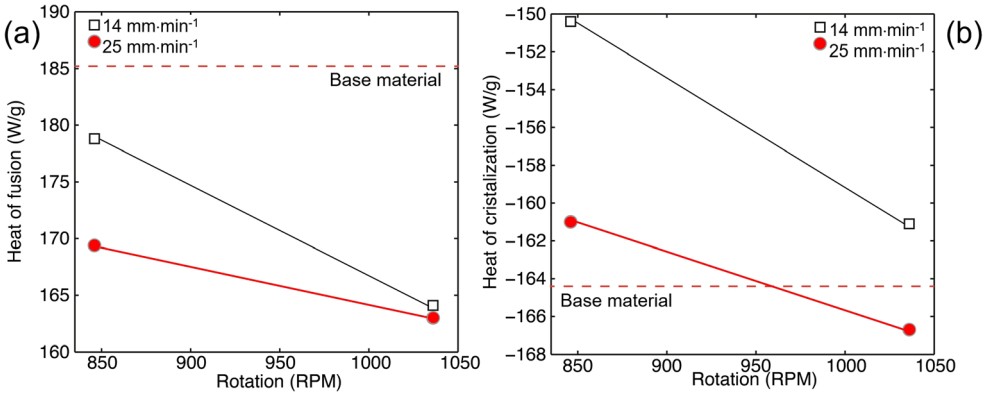

Fig. 14 Effect of rotation speed for two different welding speeds on **a** fusion heat and **b** HDPE crystallization

3.4 DSC results and material flow

The thermal effects generated during the welding process of the samples can be shown quantitatively comparing the specific properties of the material for the first heating, as well during the first cooling and the second heating. Figure 13 summarizes crystallinity measurements of welded samples and base material (noted as BM on Fig. 13), which were obtained from DSC experiments. The first heating (first scan) corresponds to the effect of the welding on the material. The crystallinity decreases in the stir region compared to the base material, which is consistent with prior works [13]. Second heating (second scan) shows a progressive reduction of crystallinity within stir region, when welding and rotational speeds increase.

Fusion heat for second heating and crystallization heat for intermediate cooling vs. process parameters are shown in Fig. 14a, b, respectively. In Fig. 13, the results of first heating show that the welding process did not induce significant changes in crystallinity (reduction < 10%) compared to the base material, i.e., crystallinity in the stir region remained virtually similar. According to Fig. 14a, the fusion heat decreases as welding and rotational speed values increase. This can be explained by means of the effect of heat penetration on the contact surface.

For a specific rotational speed value, if the tool passes faster, heat penetration is lower, affecting fewer crystalline zones. With slower welding speed, the molecular chains absorb more heat, which eventually eliminates crystalline zones. Although HDPE is a crystallizable thermoplastic, this research did not find evidence of recrystallization. The decreasing values in the second heating can be explained by changes in the molecular structure from the first heating to the second, i.e., a physical change, presumably due to thermal degradation of the sample. Unfortunately, this cannot be quantifiable using this technique; therefore, it is an interesting topic for further research.

4 Conclusions

- The effects of process parameters on the tensile strength and hardness, and crystallinity in HDPE welded joints using FSW and a non-rotational shoulder tool were established.
- An operational window process among 1036 to 846 rpm, and 14 to 25 mm min^{-1} of rotational and welding speed, respectively, producing welded joints free of discontinuities and overheating in the stir region.
- Hardness distribution across welded joint was more strongly affected by rotational speed; however, the effect of the welding speed on this behavior was weaker.
- Combination of welding and rotational speed was the main parameter that affected molecular structure in welded joints and, consequently, the tensile testing results.
- Crystallinity of stir region was reduced approximately 12% when rotational and welding speed were increased because of physical changes in the polymer structure produced by heat transfer and the material flow during welding process.
- Further research must be oriented to measure level of molecular degradation in welding region using DSC techniques and heating assisting welding, testing other different process parameters.

Acknowledgments The authors wish to thank Universidad Autónoma del Caribe for its financial support for this research through project CONV-I-004-P012. Special thanks to Dr. Juan F. Santa (ITM) and MSc. Ricardo Mendoza for their selfless and meaningful help with some measurements and fruitful discussions.

References

1. Nandan R, DebRoy T, Bhadeshia HKDH (2008) Recent advances in friction-stir welding–process, weldment structure and properties. Prog Mater Sci 53(6):980–1023
2. Mishra RS, Ma ZY (2005) Friction stir welding and processing. Mat Sci Eng R 50(1):1–78
3. Rajamanickam N, Balusamy V, Reddy GM, Natarajan K (2009) Effect of process parameters on thermal history and mechanical properties of friction stir welds. Mater Design 30(7):2726–2731
4. Thomas WM, Nicholas ED, Needham JC, Murch MG, Temple-Smith P, Dawes, CJ (1995) Friction welding. U.S. patent no. 5460317A. Washington, DC: US Patent and Trademark Office
5. Threadgill PL, Leonard AJ, Shercliff HR, Withers PJ (2013) Friction stir welding of aluminium alloys. Inter Mater Rev 54(2): 49–93
6. Throughton M (2008) In: handbook of plastics joining, 2nd edn. William Andrew Inc., England
7. Peacock A (2000) Handbook of polyethylene: structures: properties, and applications. Marcel Dekker inc, New York
8. Vijayan V, Pokharel P, Kang MK, Choi S (2016) Thermal and mechanical properties of e-beam irradiated butt-fusion joint in high-density polyethylene pipes. Radiat Phys Chem 122:108–116
9. Lai HS, Kil SH, Yoon KB (2015) Effects of defect size on failure of butt fusion welded MDPE pipe under tension. J Mech Sci Technol 29(5):1973–1980
10. Leskovics K, Kollár M, Bárczy P (2006) A study of structure and mechanical properties of welded joints in polyethylene pipes. Mat Sci Eng A-Struct 419(1):138–143
11. Li H, Gao B, Dong J, Fu Y (2016) Welding effect on crack growth behavior and lifetime assessment of PE pipes. Polym Test 52:24–32
12. Grewell DA, Benatar A, Park JB (2003) Plastics and composites welding handbook v 10. Hanser Gardner, Munich
13. Kiss Z, Czigány T (2007) Applicability of friction stir welding in polymeric materials. Period Polytech Mech Eng 51(1):15–18
14. Hoseinlaghab S, Mirjavadi SS, Sadeghian N, Jalili I, Azarbarmas M, Givi MKB (2015) Influences of welding parameters on the

quality and creep properties of friction stir welded polyethylene plates. Mater Design 67:369–378
15. Bozkurt Y (2012) The optimization of friction-stir welding process parameters to achieve maximum tensile strength in polyethylene sheets. Mater Design 35:440–445
16. Nateghi E, Hosseinzadeh M (2016) Experimental investigation into effect of cooling of traversed weld nugget on quality of high-density polyethylene joints. Int J Adv Manuf Tech 84(1–4):581–594
17. Azarsa E, Mostafapour A (2014) Experimental investigation on flexural behavior of friction stir welded high-density polyethylene sheets. J Manuf Proc 16(1):149–155
18. Banjare PN, Sahlot P, Arora A (2017) An assisted heating tool design for FSW of thermoplastics. J Mat Proc Tech 239:83–91
19. Vijendra B, Sharma A (2015) Induction heated tool assisted friction-stir welding (i-FSW): a novel hybrid process for joining of thermoplastics. J Manuf Proc 20:234–244
20. Simões F, Rodrigues DM (2014) Material flow and thermo-mechanical conditions during friction stir welding of polymers: literature review, experimental results and empirical analysis. Mater Design 59:344–351
21. Pirizadeh M, Azdast T, Ahmadi SR, Shishavan SM, Bagheri A (2014) Friction stir welding of thermoplastics using a newly designed tool. Mater Design 54:342–347
22. Rezgui MA, Ayadi M, Cherouat A, Hamrouni K, Zghal A, Bejaoui S (2010) Application of Taguchi approach to optimize friction stir welding parameters of polyethylene. In EPJ web of conferences vol. 6, p. 07003. EDP Sciences. DOI:https://doi.org/10.1051/epjconf/20100607003
23. Inaniwa S, Kurabe Y, Miyashita Y, Hori H (2014) Application of friction stir welding for several plastic materials. In Proceedings of the 1st International Joint Symposium on Joining and Welding: Osaka, Japan, pp. 137
24. Kleijnen JP (2008) Design and analysis of simulation experiments, vol. 20. Springer, New York
25. Balart R, López J, García PF (2003) Técnicas experimentales de análisis térmico de polímeros. University books MD, Madrid
26. American Standard Tests and Measurements (2014) ASTM D638 - 14 standard test method for tensile properties of plastics. West Conshohocken. https://www.astm.org/Standards/D638.htm
27. Kiss Z, Czigany T (2012) Microscopic analysis of the morphology of seams in friction stir welded polypropylene. Express Polym Lett 6(1):54–62
28. Dowling NE (2007) Mechanical behaviour of materials: engineering methods for deformation, fracture and fatigue, 3rd ed. Prentice Hall, London